Chemistry–A European Journal
Research Article
doi.org/10.1002/chem.202500807
Chemistry Europe
European Chemical Societies Publishing
www.chemeurj.org

Dissecting the Diverse Reactivity of β-Diketiminate Aluminum(I) Compound towards Azaarenes: Insight From DFT Calculations

Ka Lok Chan,[a] Pak Fung Lau,[a] and Zhenyang Lin*[a]

Interest in aluminum(I) complexes has surged in recent decades due to the unusual role of electropositive aluminum as donor atoms in ligands. Numerous Al(I) complexes, which were previously considered too unstable, have been isolated. Among these, β-diketiminate aluminum(I) complex, NacNacAl(I), stands out for its unique reactivities including oxidative addition and π-bond activation. However, the understanding of reactions involving NacNacAl(I) has not yet been fully established. This study unveils the mechanisms behind the diverse reactivity of NacNacAl(I) with five structurally similar azaarenes through DFT calculations. Interestingly, computational results indicate that some of the five reactions can proceed via radical processes. A holistic comparison of all results highlights the mechanistic differences between monocyclic and bicyclic azaarenes. In the initial step with NacNacAl(I), monocyclic azaarenes form Al(I)-azaarene adducts, whereas bicyclic azaarenes generate Al(II)-azaarene biradicals. These intermediates are critical for understanding their distinctive reactivity. For monocyclic azaarenes, electronic effects of their substituents on the azaarene adducts result in varying reaction outcomes, while for bicyclic azaarenes, subsequent intermolecular or intramolecular coordination of biradicals leads to different products. This study provides deeper mechanistic insights into reactions associated with NacNacAl(I) complexes, thereby contributing to a more comprehensive understanding of these reactions.

1. Introduction

Recently, there has been a notable surge in enthusiasm surrounding aluminum(I) complexes. This newfound interest can be attributed to the unconventional role of the electropositive aluminum as a donor atom of a ligand, which is highly unusual and unexpected. These complexes, characterized by an aluminum center with a +1 oxidation state rather than the most common states of 0 and +3, were previously deemed thermodynamically unstable and therefore challenging to synthesize until the isolation of stable compounds such as the first molecular Al(I) complex, $[(AlCp^*)_4]$ (Cp^*=C_5Me_5, **I**, Figure 1)[1] and the first monomeric Al(I) complex, NacNacAl(I) (NacNac=[DippNC(Me)CHC(Me)NDipp]$^-$, Dipp = 2,6-^{i}Pr$_2$C$_6$H$_3$, **II**, Figure 1).[2] Following these notable discoveries, chemists have been actively synthesizing novel neutral monomeric Al(I) complexes[3–9] and carrying out extensive experimental[10–25] and theoretical studies[26–31] on them. Alongside these studies, it is also imperative to emphasize the growing prominence of anionic Al(I) chemistry[29,32–36] in recent research, which plays a pivotal role in advancing Al(I) chemistry.

Among the numerous neutral monomeric Al(I) complexes, the above-mentioned NacNacAl(I) complex stands out as one of the most extensively researched. This NacNacAl(I) complex has been described as an Al(I) complex akin to a carbene analogue.[2] It has displayed a spectrum of unusual reactivities. Analogous to a transition metal, it can also undergo oxidative addition of σ-bonds, including H—X (X=H, Si, B, Al, C, N, P),[27,37,38] C—F, and C—O bonds,[21,28,39–41] as well as S—S, P—P, and S—C bonds.[42] Functioning as a carbenoid, it can activate π-bonds of azobenzene,[43] olefin,[28,44] acetylene,[45,46] and guanidine.[47] Recent reports have also highlighted the NacNacAl(I) complex's capability to engage in pericyclic reactions with dienes, aromatic systems,[48] and even C_{60} clusters.[49]

In this work, we are interested in the recently reported reactions of this carbenoid with structurally similar azaarenes.[50] In these reactions, as illustrated in Scheme 1, the NacNacAl(I) complex exhibited a wide range of reactivities, including the oxidation addition involving the aromatic C(4)—H bond in 3,5-lutidine to form **LUT_P**, the deprotonation of the methyl substituent of 4-picoline to yield **PIC_P**, the deprotonation at the β-methyl position of the NacNac backbone upon reaction with 4-Dimethylaminopyridine (DMAP) resulting in **DMAP_P**, the C(2)—C(2) coupling between two quinoline molecules to produce **QUI_P**, and the cleavage of the N—N bond in phthalazine to give **PHT_P**.

[a] K. L. Chan, P. F. Lau, Z. Lin
Department of Chemistry, The Hong Kong University of Science and Technology, Clear Water Bay, Kowloon, Hong Kong, People's Republic of China
E-mail: chzlin@ust.hk

Ka Lok Chan and Pak Fung Lau contributed equally to this work.

Supporting information for this article is available on the WWW under https://doi.org/10.1002/chem.202500807

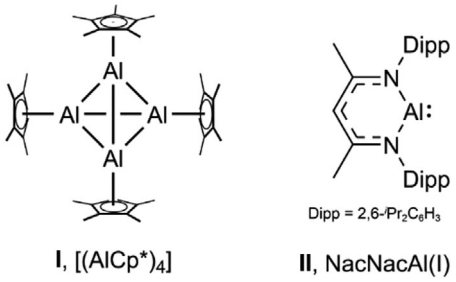

Figure 1. First examples of stable Al(I) complexes.

Inspired by the fascinating experimental findings presented in Scheme 1, we are compelled to delve into the underlying mechanisms that govern these substrate-controlled reactions. Through this exploration, we aim to address the following important scientific questions: (i) the origins of the varied reactivity of NacNacAl(I) and (ii) the effects of different azaarenes in these reactions. In this work, we attempt to attain a holistic theoretical understanding of the diverse reactivity through systematic density functional theory (DFT) calculations. We hope the findings will provide valuable insights into the mechanistic understanding in the field of Al(I) chemistry.

2. Results and Discussion

2.1. Reactions of NacNacAl(I) with Monocyclic Azaarenes: Two-Electron Pathways

As mentioned in the Introduction, NacNacAl(I) resembles a singlet carbene, with a filled sp^2-hybridized orbital and a vacant p orbital, allowing the Al center to behave both as a Lewis acid and a Lewis base. Numerous studies have revealed that NacNacAl(I) is an ambiphilic carbenoid isoelectronic with carbene and is capable of engaging in a one-step oxidative addition of σ-bonds.[51] However, we found that upon reacting with azaarenes, NacNacAl(I) utilizes its vacant p orbital to first form an adduct by coordinating with the N atom of the basic azaarenes. Upon the coordination of the N atom of azaarene to the vacant Al p orbital of NacNacAl(I), the hybridization of the orbital that hosts the lone pair electrons of Al(I) changes from sp^2 to sp^3, which features a decrease in the s-character of the orbital hosting the lone pair of electrons, greatly enhancing the nucleophilicity and basicity of the NacNacAl(I) complex. Hence, the coordination of the N atom of azaarene to the vacant Al p orbital of NacNacAl(I) serves as a crucial step for the pre-activation of the NacNacAl(I) complex, which enables a highly nucleophilic or basic adduct to undergo numerous challenging reactions such as nucleophilic attack on an aromatic system of 3,5-lutidine

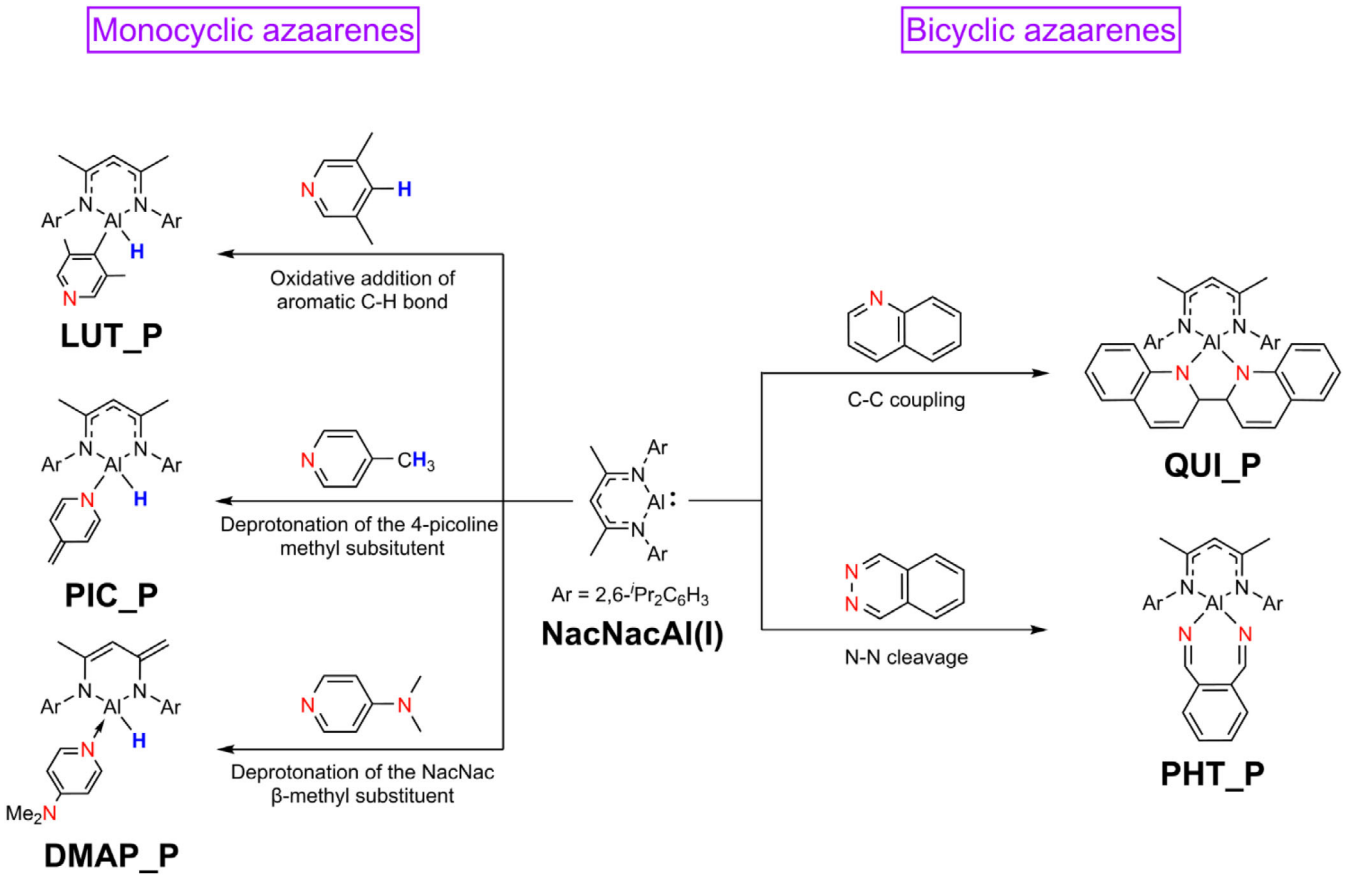

Scheme 1. Reactions of NacNacAl(I) with 3,5-lutidine (**LUT**), 4-picoline (**PIC**), 4-dimethylaminopyridine (**DMAP**), quinoline (**QUI**) and phthalazine (**PHT**).

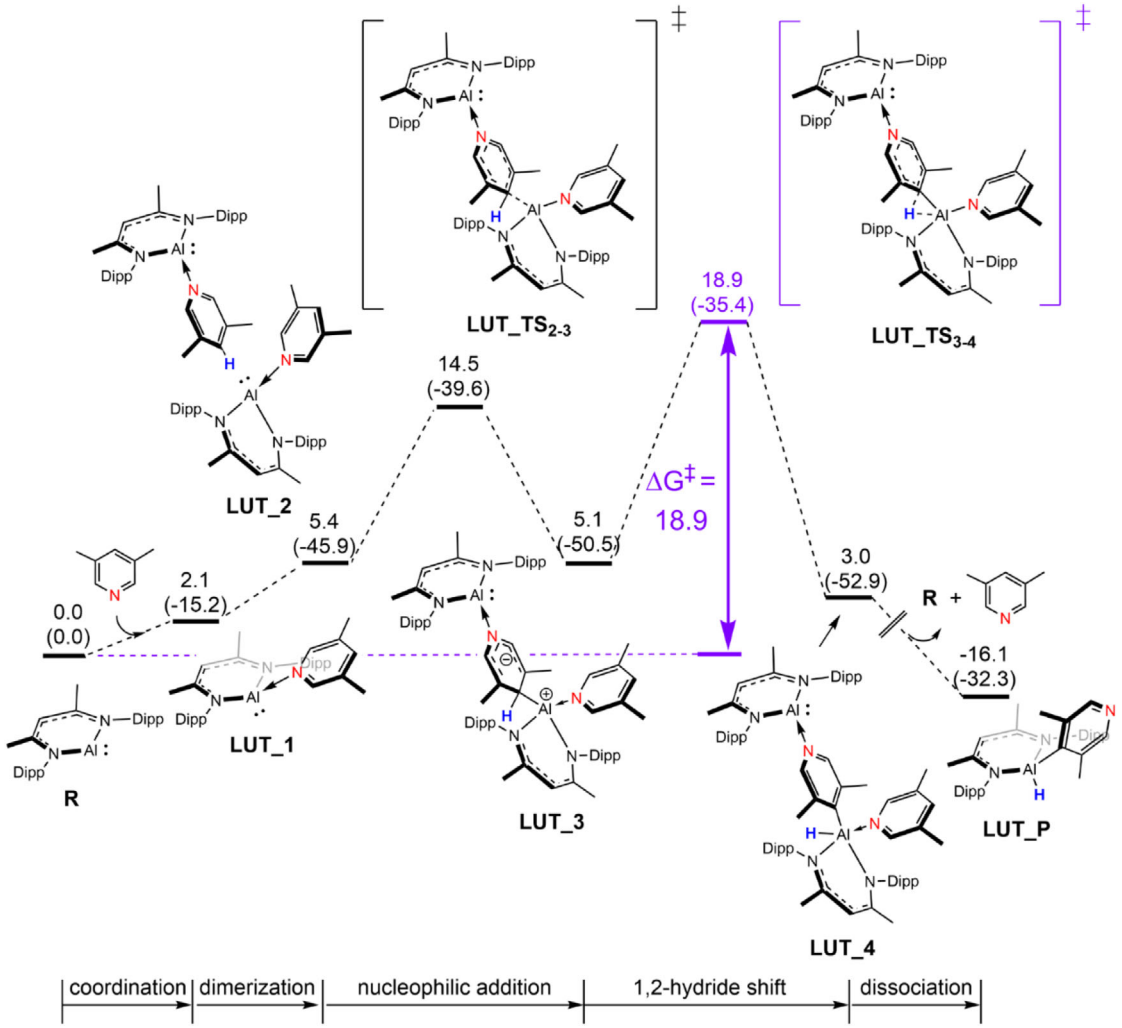

Figure 2. Energy profile calculated for the reaction of NacNacAl(I) with 3,5-lutidine. Relative free energies and electronic energies (in parentheses) are given in kcal/mol.

(Section 2.1.1), deprotonation of the methyl substituent from 4-picoline (Section 2.1.2) and deprotonation at the β-methyl position of the NacNac backbone upon reaction with DMAP (Section 2.1.3).

2.1.1. Oxidative addition of aromatic C(4)-H bond of 3,5-lutidine (LUT)

As previously mentioned, 3,5-lutidine first coordinates with NacNacAl(I) to form the 3,5-lutidine-coordinated adduct **LUT_1** (Figure 2). Upon coordination, the nucleophilicity of the lone pair electrons on the Al atom of the adduct is greatly enhanced. Then, two molecules of **LUT_1** form the van der Waals dimer species **LUT_2**, with the H on the C(4) position of one adduct pointing towards the lone pair of electrons on the Al atom of the other adduct. In such a conformation, the orbital accommodating the lone pair of electrons on the Al atom of the second adduct is ready to interact with the π^* orbital at the C(4) position of the 3,5-lutidine of the first adduct. Next, the highly nucleophilic lone pair of electrons of the second adduct undergoes nucleophilic attack on the C(4) position of the coordinated 3,5-lutidine in the first adduct, resulting in a dearomatization of 3,5-lutidine in the first adduct. The dearomatization process is facilitated by two factors, which are the high nucleophilicity of the lone pair of electrons in the first adduct and the electron-withdrawing ability of the NacNacAl(I) moiety in the second adduct. The high nucleophilicity of the lone pair of electrons enables an easier nucleophilic attack on the 3,5-lutidine ring, while the electron-withdrawing NacNacAl(I) moiety in the second adduct makes the 3,5-lutidine more electrophilic and withdraws the excess negative charge built on the 3,5-lutidine ring after dearomatization process, thus stabilizing the formed zwitterion **LUT_3**. **LUT_3** then undergoes a 1,2-hydride shift from the electron-rich bridging lutidine moiety to the newly-formed electron-deficient Al(III) center, yielding the hypervalent species **LUT_4**. As the 1,2-hydride shift involves an arene C—H bond cleavage, it is the rate-determining step of the reaction with an overall free-energy barrier of 18.9 kcal/mol. Following this rate-determining step, a sequential dissociation of one molecule of NacNacAl(I) and one molecule of 3,5-lutidine from **LUT_4** generates the final experimentally-observed Al(III) product **LUT_P**.

We also examined alternative pathways that do not involve the van der Waals dimer species **LUT_2**. Figure 3a shows the energy profile associated with the nucleophilic attack of the 3,5-lutidine-coordinated adduct **LUT_1** on the C(4) position of a free 3,5-lutidine molecule. The resulting energy barrier is 29.8 kcal/mol, which is significantly higher than that (18.9 kcal/mol) presented in Figure 2. Thus, it suggests that NacNacAl(I) moiety in the 3,5-lutidine-coordinated NacNacAl(I) plays a crucial role in enhancing the electrophilicity of the 3,5-lutidine ring and hence facilitating the dearomatization process, as shown in Figure 2. Figure 3b shows the energy profile for the nucleophilic attack on the C(4) position of the lutidine moiety in the 3,5-lutidine-coordinated NacNacAl(I) by the uncoordinated NacNacAl(I) through **LUT_TS**$_{7\text{-}8}$. The corresponding energy barrier reaches 47.5 kcal/mol, which is inaccessibly high. It demonstrates that the pre-coordination of 3,5-lutidine on the NacNacAl(I) complex before undergoing nucleophilic attack is also crucial for enhancing the nucleophilicity of the lone pair of electrons for the dearomatization process to proceed. Figure 3c shows the energy profile for a one-step direct oxidative addition of the C(4)—H bond of a free 3,5-lutidine to NacNacAl(I). The resulting energy barrier reaches 57.1 kcal/mol, which is also inaccessibly high. It indicates that such a one-step pathway is highly unlikely, due to the relatively low nucleophilicity of the NacNacAl(I) lone pair of electrons prior to the coordination of azaarene and the relatively low electrophilicity of the 3,5-lutidine ring before its coordination to NacNacAl(I).

2.1.2. Deprotonation of the methyl group of 4-picoline (PIC)

In the case of 4-picoline, the C(4) position of the N-heteroarene ring is substituted by a methyl group, instead of an H atom in 3,5-lutidine. As the oxidative addition of C—C bond in 4-picoline is much more challenging than that of C—H bond in 3,5-lutidine, the NacNacAl(I) complex would attack an alternative site that is more reactive. As the deprotonation of methyl substituent of the 4-picoline could yield a product with the negative charge localized on the electronegative N atom of 4-picoline in its resonance structure, the NacNacAl(I) complex preferentially acts as a Brønsted base, instead of a nucleophile, to deprotonate the methyl substituent.

Figure 4 shows the energy profile calculated for the reaction between NacNacAl(I) and 4-picoline. Again, the first step of the reaction is the adduct formation through the coordination of 4-picoline to NacNacAl(I). This greatly enhances the basicity of the lone pair on the Al(I) center. Once the adduct **PIC_1** is formed, similar to what we discussed above in the reaction of 3,5-lutidine, two molecules of **PIC_1** combine to form the van der Waals dimer species **PIC_2**. In this van der Waals dimer species, a C-H bond on the methyl group of the coordinated 4-picoline in one adduct monomer is directed towards the lone pair of the Al(I) center in the other, accompanied by π—π stacking between the two azaarene moieties. Subsequently, one adduct utilizes its basic lone pair of electrons on the Al(I) center to abstract a proton from the methyl group of the 4-picoline moiety in another, generating the ion pair **PIC_3**, with an Al(III) metal center in the cation and an Al(I) metal center in the anion. As the transition state **PIC_TS**$_{2\text{-}3}$ in this step involves a disruption of aromaticity, it is the rate-determining transition state of the reaction. Similar to the case with 3,5-lutidine, there are also two factors facilitating the deprotonation process of 4-picoline, which are the higher basicity of the lone pair of electrons on the Al(I) center upon adduct formation and the electron-withdrawing ability of the NacNacAl(I) moiety in the adduct being deprotonated. The former factor ensures that the adduct is more likely to deprotonate a proton and the latter factor could decrease electron density on the coordinated 4-picoline molecule, rendering the proton in methyl substituent of 4-picoline more acidic, thus facilitating the deprotonation process. From **PIC_3**, a similar deprotonation process occurs, generating two molecules of the products in the form of a van der Waals dimer, designated as **PIC_4**. Finally, the van der Waals dimer **PIC_4** dissociates, yielding two molecules of the monomeric product **PIC_P**.

To explore whether the pre-coordination of 4-picoline on NacNacAl(I) is crucial for the deprotonation of methyl group in 4-picoline in the van der Waals' dimer **PIC_2**, we also examined the direct deprotonation of a 4-picoline methyl C-H bond utilizing the 4-picoline-coordinated NacNacAl(I) **PIC_1** (Figure 5a). Similar to what we found in the case of 3,5-lutidine, this pathway also has a significantly higher barrier of 26.4 kcal/mol than that (20.8 kcal/mol) presented in Figure 4 through the van der Waals dimer species **PIC_2**, demonstrating that the pre-coordination of 4-picoline on NacNacAl(I) facilitates the deprotonation.

Direct oxidative addition of a 4-picoline methyl C—H σ-bond to NacNacAl(I) is also examined. As depicted in Figure 5b, this pathway starts with a one-step C—H bond oxidative addition through **PIC_TS**$_{R\text{-}6}$ which produces the Al(III) intermediate **PIC_6**. Subsequently, the intermediate **PIC_6** undergoes 1,3 migration through the intermediate **PIC_7** to yield the product **PIC_P**. Alternatively, the intermediate **PIC_7** can also be formed through a C—H activation process through **PIC_TS**$_{R\text{-}7}$. However, both pathways have inaccessibly high energy barriers for the formation of the intermediate **PIC_6** or **PIC_7** through the one-step oxidative addition (**PIC_TS**$_{R\text{-}6}$) or the C-H activation process (**PIC_TS**$_{R\text{-}7}$), due to the low basicity of NacNacAl(I) and the low acidity of the methyl C-H bonds in 4-picoline.

2.1.3. Deprotonation of the β-methyl group at the ligand backbone of NacNacAl(I) by DMAP

4-Dimethylaminopyridine (DMAP) closely resembles 4-picoline both structurally and electronically. Structurally, as DMAP, similar to 4-picoline, has the C(4) position substituted, the C(4) position is not available for nucleophilic attack. Electronically, as both DMAP and 4-picoline have electron-donating groups substituted at the *para*-position, one might expect that their chemistry towards NacNacAl(I) should closely resemble each other. However, the —NMe_2 substituent on DMAP lacks protons that are sufficiently acidic to engage in deprotonation reactions, in contrast to the presence of an acidic proton on methyl group substituent of 4-picoline, which undermines the ability of DMAP to function as a Brønsted acid for deprotonation. Thus, NacNacAl(I) has to react with another acidic site in the reaction with DMAP. In light of this, Arnold and coworkers reported that the

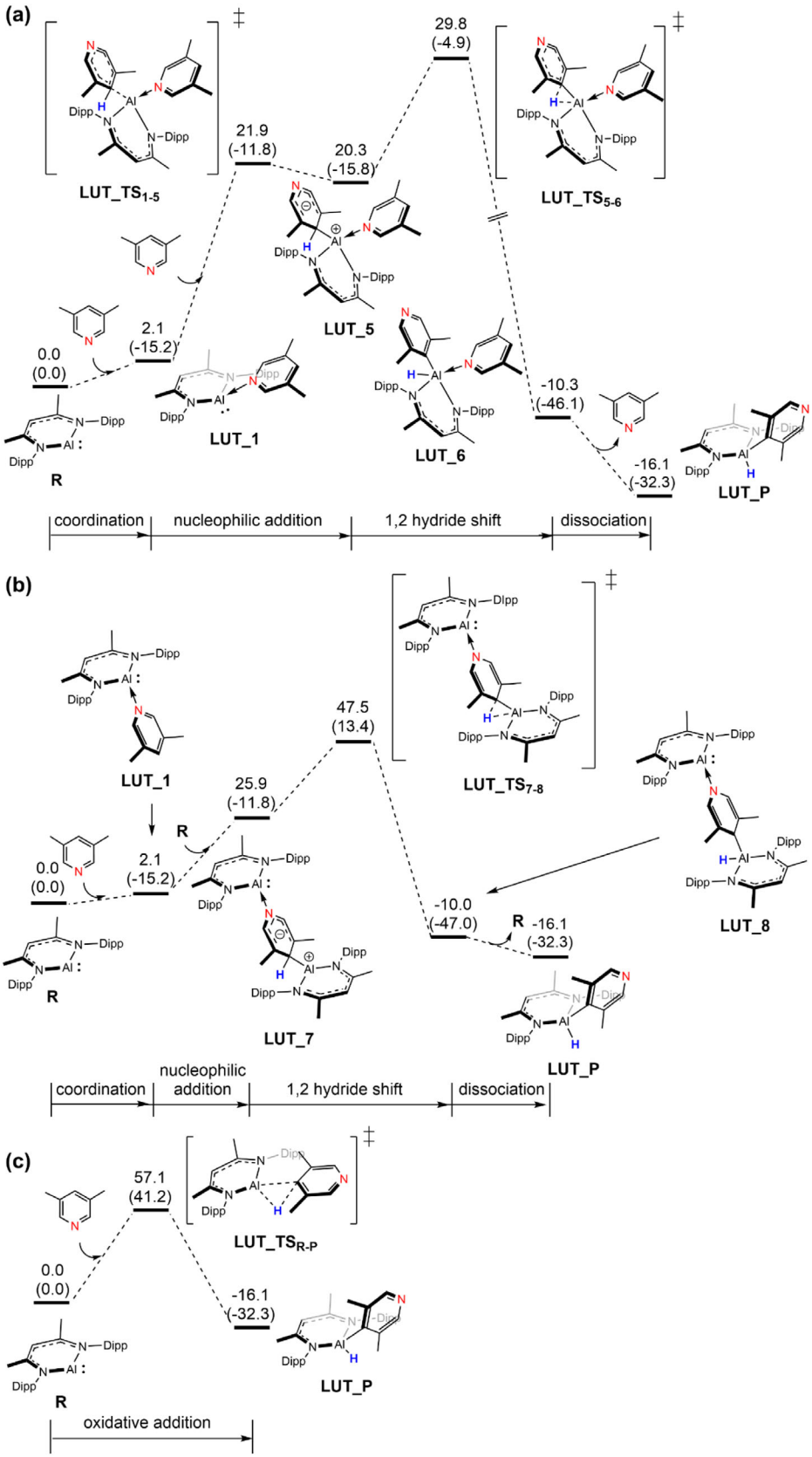

Figure 3. Energy profiles of other less favorable pathways for the reaction of NacNacAl(I) with 3,5-lutidine: (a) nucleophilic attack on the C(4) position of a free 3,5-lutidine molecule by 3,5-lutidine-coordinated NacNacAl(I), (b) nucleophilic attack on the C(4) position of the 3,5-lutidine moiety in the 3,5-lutidine-coordinated NacNacAl(I) by uncoordinated NacNacAl(I) and (c) oxidative addition of the C(4)—H bond of 3,5-lutidine. Relative free energies and electronic energies (in parentheses) are given in kcal/mol.

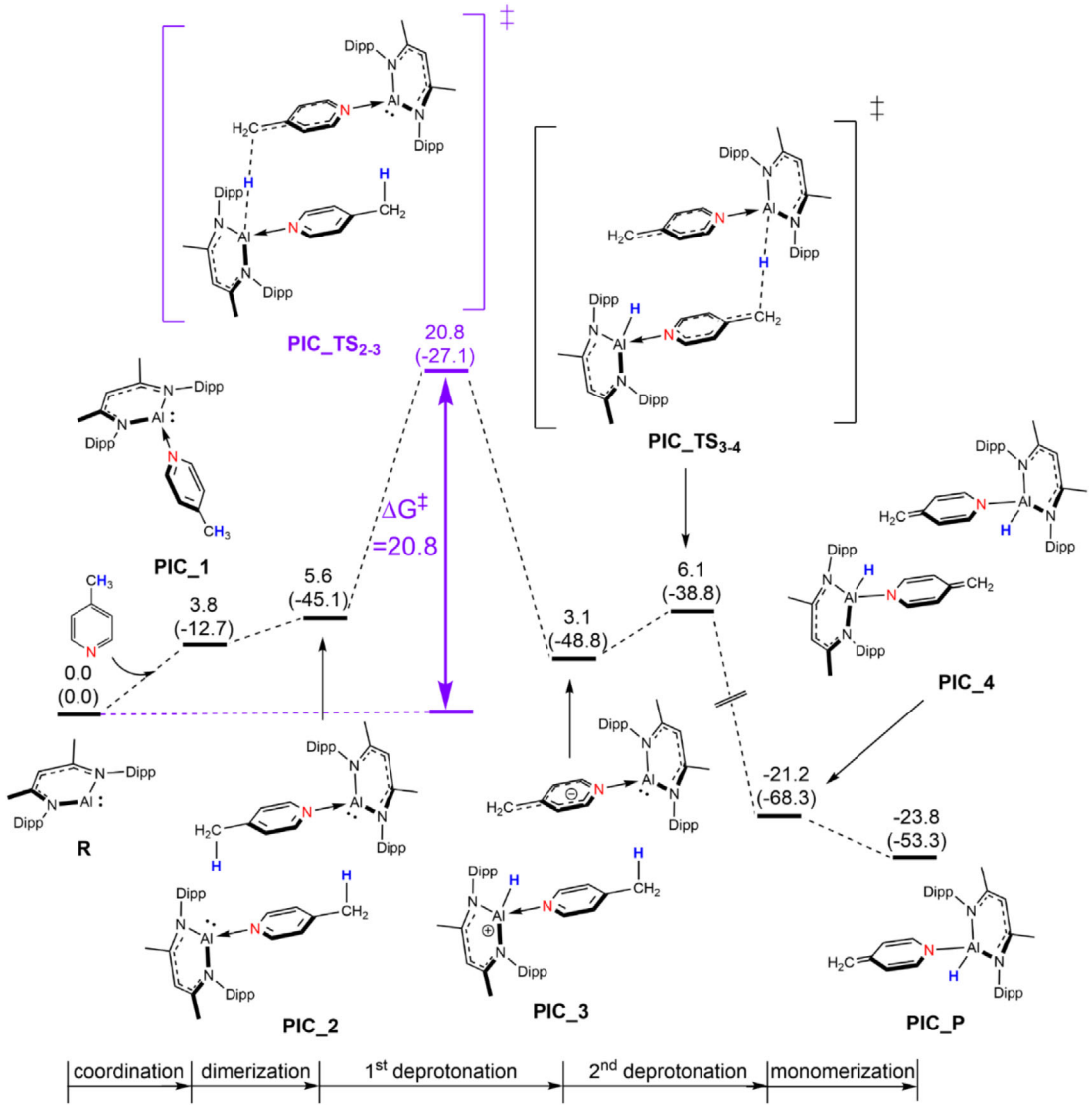

Figure 4. Energy profile calculated for the proposed pathway for the reaction of NacNacAl(I) with 4-picoline yielding 2 molecules of products. Relative free energies and electronic energies (in parentheses) are given in kcal/mol.

β-methyl group in the NacNac backbone features reasonably acidic C-H bonds, which can undergo deprotonation in the presence of a strong base,[52] and Nikonov and coworkers published a reaction involving deprotonation of the β-methyl group in the NacNac backbone using urea as the base.[53] Thus, as no reasonably electrophilic or acidic sites are available in DMAP, the NacNacAl(I)-DMAP adduct deprotonates the β-methyl group in the NacNac backbone of NacNacAl(I).

The energy profile calculated for the favorable pathway of deprotonation of the β-methyl group in the NacNac backbone is shown in Figure 6. Similar to the case with 3,5-lutidine and 4-picoline, DMAP also firstly coordinates with NacNacAl(I) to generate a Lewis base adduct **DMAP_1**, which renders the lone pair on the Al(I) center highly basic. Then, the Al(I) lone pair of the NacNacAl(I)-DMAP adduct abstracts a proton from the β-carbon (C_β) in the NacNac backbone of the uncoordinated NacNacAl(I) through **DMAP_TS$_{1\text{-}2}$**, leading to the formation of **DMAP_2**, an ion pair comprising an Al(III)-hydride cation and an anion having an Al(I) center. The main reason why the Al(I) lone pair abstracts the proton from an uncoordinated NacNacAl(I), instead of a coordinated one, is due to the fact that the coordination of DMAP on Al(I) would increase the electron density of the NacNac backbone, rendering the hydrogen at C_β less acidic. The transition state **DMAP_TS$_{1\text{-}2}$** is the rate-determining TS with a barrier of 18.5 kcal/mol. Subsequently, the anion in the ion pair coordinates with another free DMAP molecule, forming a new ion pair **DMAP_3** to increase the basicity of the Al(I) lone pair. The two ions in **DMAP_3** then undergo a spatial reorientation, where the hydrogen at the C_β atom of NacNac in the cation is closer to the lone pair of the Al(I) center in the anion, forming a more thermodynamically stable ion pair designated as **DMAP_4**. Such reorientation sets the stage for the second deprotonation step, which is an almost barrierless process leading to the formation of the van der Waals dimer species **DMAP_5**. In **DMAP_4**, the adduct consisting of Al(I) lone pair is negatively charged and the adduct subjected to deprotonation is positively charged.

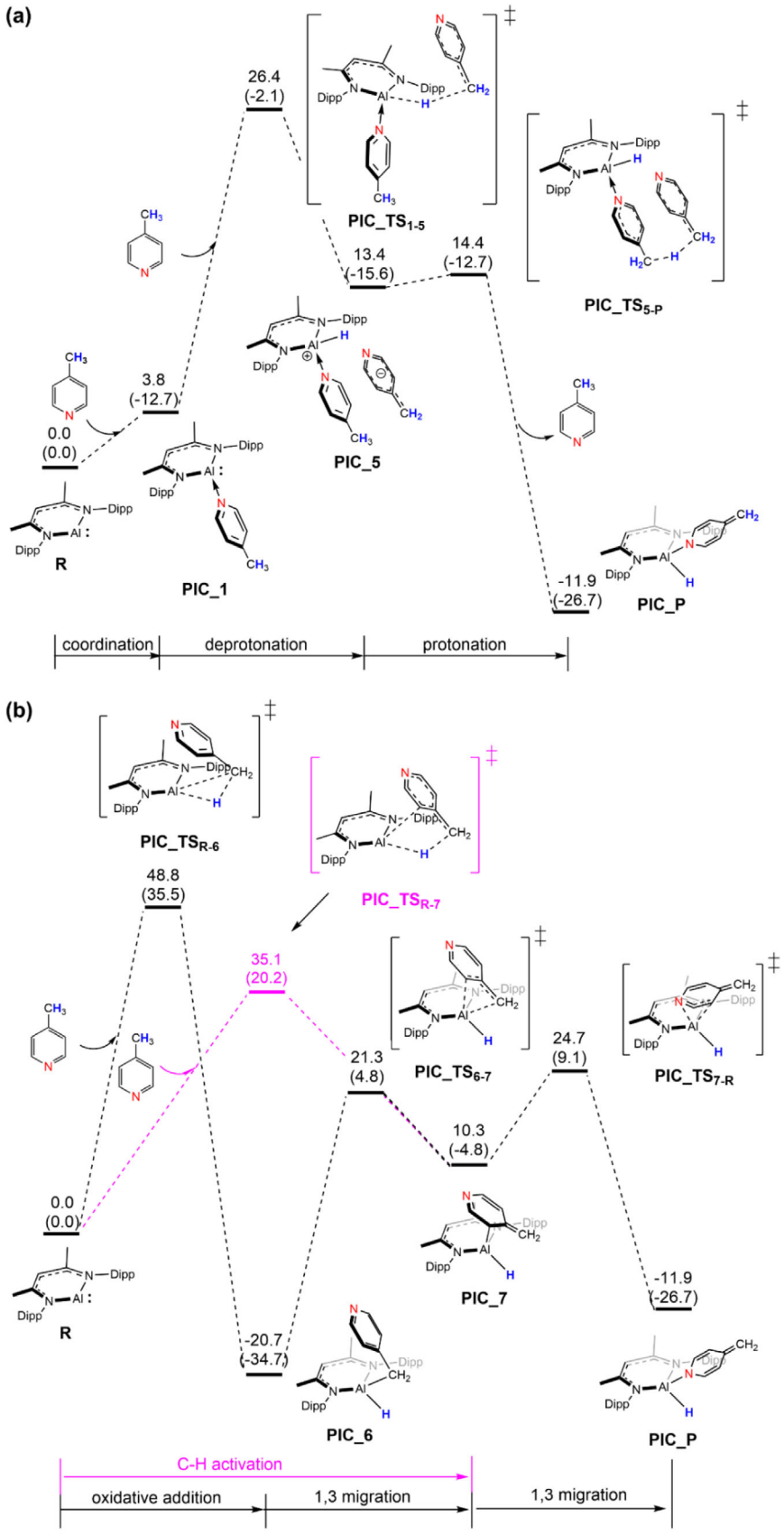

Figure 5. Energy profiles of other less favorable pathways for the reaction of NacNacAl(I) with 4-picoline: (a) direct deprotonation of a 4-picoline methyl C—H bond utilizing **PIC_1**, the 4-picoline-coordinated NacNacAl(I) and (b) oxidative addition of a 4-picoline methyl C—H bond. Relative free energies and electronic energies (in parentheses) are given in kcal/mol.

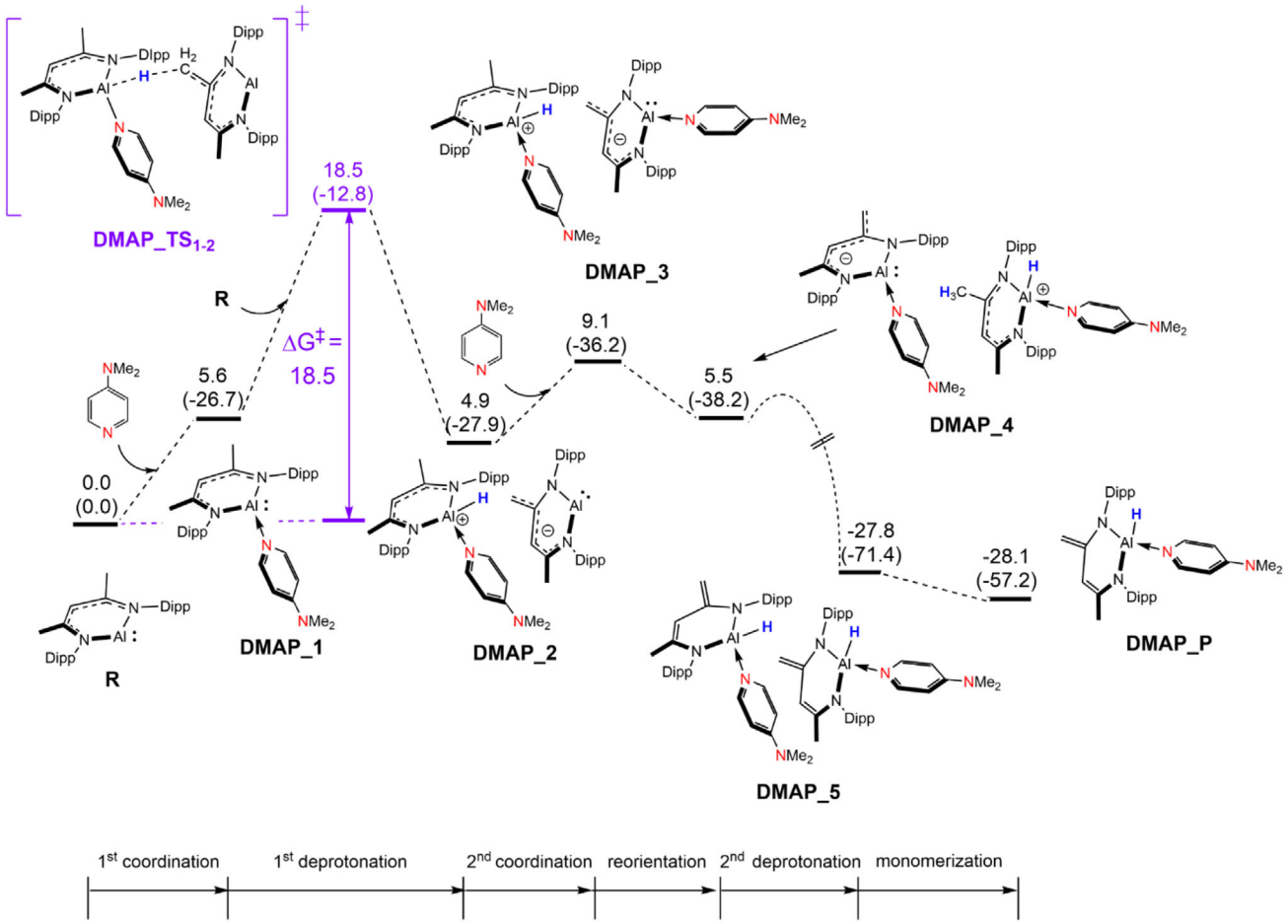

Figure 6. Energy profile calculated for the proposed pathway for the reaction of NacNacAl(I) with DMAP yielding two molecules of products. Relative free energies and electronic energies (in parentheses) are given in kcal/mol.

Therefore, the second deprotonation in **DMAP_4** proceeds with almost no energy barrier. Finally, this dimer quickly monomerizes to yield the neutral Al(III) product **DMAP_P**.

Figure 7 shows the energy profile calculated for the less favorable pathway of deprotonation of the C_β—H σ-bond in the NacNacAl(I)-DMAP adduct by another NacNacAl(I)-DMAP adduct. The energy barrier here is 24.0 kcal/mol (**DMAP_TS**$_{6\text{-}3}$), higher than that presented in Figure 6. Clearly, the C_β—H bond in the NacNac backbone of the DMAP-coordinated NacNacAl(I) is less acidic when compared to that in NacNacAl(I). We also calculated the process of deprotonation of the C_β—H σ-bond of the uncoordinated NacNacAl(I) by free DMAP, which features a free energy change of 33.6 kcal/mol, suggesting that this process is energetically not feasible.

2.2. Reactions of NacNacAl(I) with Bicyclic Azaarenes: One-Electron Pathway

The pathways mentioned in Section 2.1 all involve two-electron processes, in which azaarene-coordinated NacNacAl(I) acts as either a strong nucleophile or base. For bicyclic azaarenes, such as quinoline and phthalazine, readers might expect that they will undergo reactions in a similar manner as the aforementioned monocyclic azaarenes. Nonetheless, surprisingly, the reactions with bicyclic azaarenes exhibit a significant twist from the monocyclic analogues, due to the more extensive conjugated π system of bicyclic azaarenes compared to monocyclic azaarenes. Thus, for bicyclic azaarenes, instead of forming a simple Lewis acid-base adduct in which the two valence electrons on Al(I) are paired in an sp^3-hybridized orbital, NacNacAl(I) undergoes a different reaction mechanism. This alternative mechanism avoids a configuration that could incur a pairing energy penalty. Specifically, when an adduct is formed with a bicyclic azaarene, NacNacAl(I) transfers one of the two valence electrons on Al(I) to the low-lying lowest-unoccupied molecular orbital (LUMO) of the π^* orbital of the extensive conjugated π system of a bicyclic azaarene. This results in the formation of a singlet biradical adduct, characterized by two non-interacting doublets with opposite spins occupying the sp^3-hybridized orbital of the Al center and the π^* orbital of the coordinated bicyclic azaarene, respectively. Singlet biradicals are recognized as key intermediates of many bond formation or cleavage processes,[54] and previous computational studies have suggested that NacNacAl(I) can react as a biradicaloid.[46,55] Indeed, our computational results indicate that the reductive coupling of two molecules

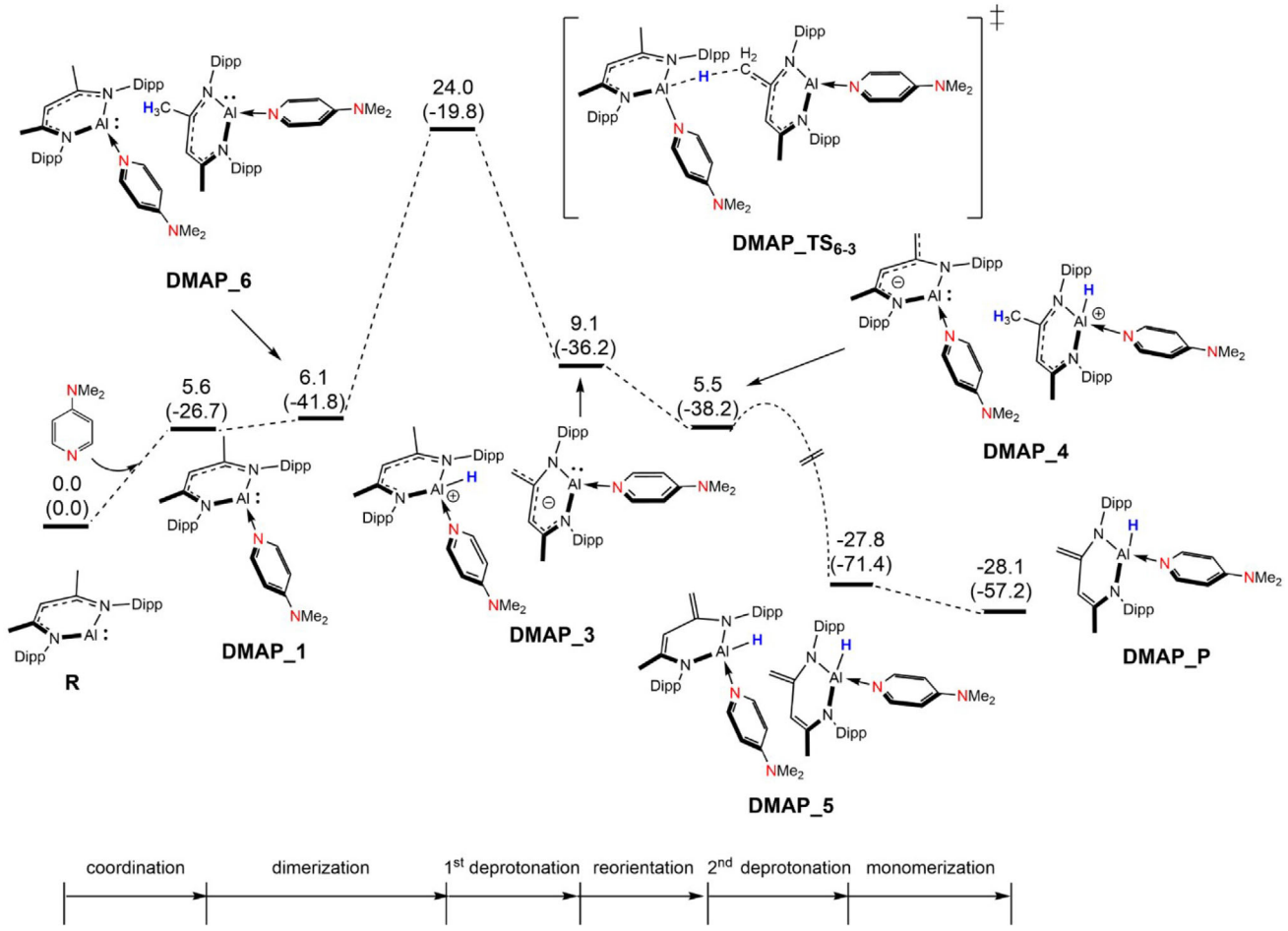

Figure 7. Energy profile calculated for an alternative pathway for the reaction of NacNacAl(I) with DMAP: deprotonation of the NacNacAl(I)-DMAP adduct by another NacNacAl(I)-DMAP adduct yielding 2 molecules of products. Relative free energies and electronic energies (in parentheses) are given in kcal/mol.

of quinoline and the N—N bond cleavage of phthalazine actually involve singlet biradical intermediates, which will be detailed below.

2.2.1. C(2)—C(2) reductive coupling between two molecules of quinoline (QUI)

As shown in Figure 8, a singlet biradical (**QUI_1**) intermediate can be readily formed by transferring one electron from the lone pair electrons on Al(I) of NacNacAl(I) to the low-lying π^* orbital of quinoline upon coordination of quinoline to NacNacAl(I). As revealed by the spin natural orbital (SNO) analysis,[56,57] the quinoline-coordinated biradical species features a pair of SNOs showing that the two unpaired electrons are distributed in the π system of the coordinated quinoline and located on the sp^3-hybridized orbital of the Al(II) center, respectively (Figure 9). Then, the Al(II) center in **QUI_1** further coordinates with a second molecule of quinoline. In the newly-formed species **QUI_2**, the unpaired electron originally located in the sp^3-hybridized orbital on the Al(II) center of **QUI_1** migrates to the π^* orbital of the newly-coordinated quinoline molecule. This transition results in a significantly more stable Al(III) singlet biradical **QUI_2**. SNO analysis reveals that the two unpaired electrons are separately delocalized in the π systems of the two coordinated-quinoline molecules, respectively (Figure S2, Supporting Information), rendering the species highly susceptible to radical coupling. Consequently, the two coordinated-quinoline moieties undergo radical coupling in a *trans* mode, forming a C—C bond and yielding the product **QUI_P$_{trans}$**.

In terms of stereoselectivity, the other possible product corresponds to the C-C coupling of quinoline in a *cis* mode. However, based on our calculation results presented in **Figure 10**, the relative free energy of **QUI_P$_{cis}$** is −24.8 kcal/mol, which is 2.1 kcal/mol and 14.7 kcal/mol higher than that of intermediate **QUI_2** and the main product **QUI_P$_{trans}$**, respectively. This indicates that it is not feasible to observe the thermodynamically unstable possible product **QUI_P$_{cis}$**.

At this juncture, readers may wonder whether a typical two-electron process described in Section 2.1 is indeed less favorable for the quinoline coupling reaction. Figure 11a shows the energy profile calculated for such a two-electron pathway. Similar to the two-electron pathway discussed for the reactions in Section 2.1, quinoline is first coordinated to NacNacAl(I) to form an adduct **QUI_3** with a more nucleophilic lone pair on the Al(I) center. This is followed by the nucleophilic attack on the quinoline at the C(8) position by the highly nucleophilic Al(I) lone pair, generating the

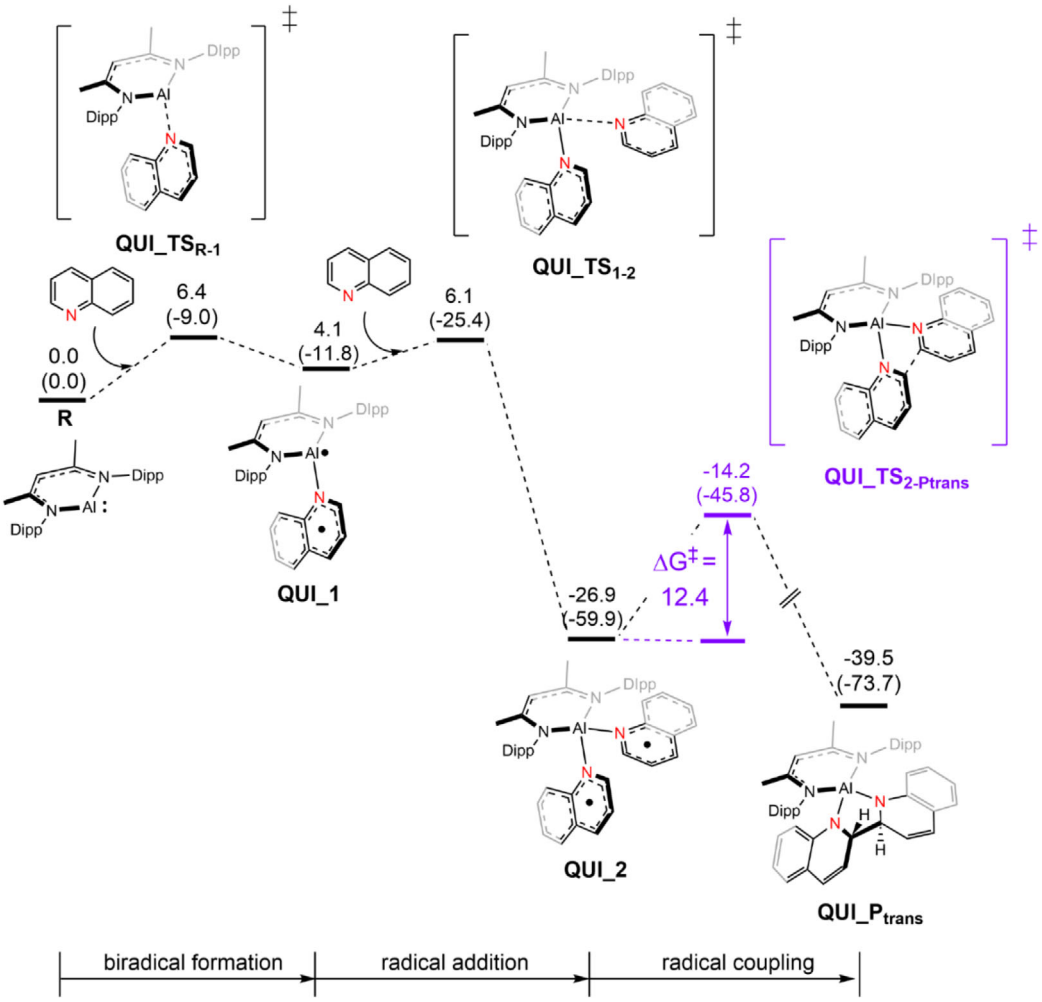

Figure 8. Energy profile calculated for the singlet biradical pathway for the reaction of NacNacAl(I) with quinoline. Relative free energies and electronic energies (in parentheses) are given in kcal/mol.

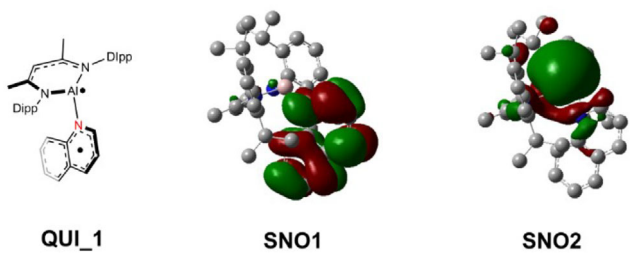

Figure 9. Spin Natural Orbitals calculated for the NacNacAl(I)-quinoline adduct **QUI_1**.

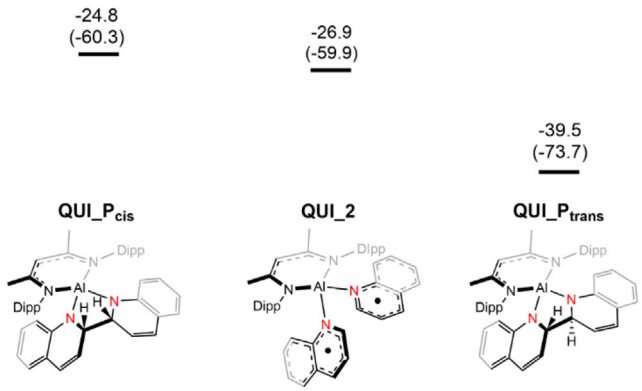

Figure 10. Relative stability among **QUI_P$_{cis}$**, **QUI_2** and **QUI_P$_{trans}$**. Relative free energies and electronic energies (in parentheses) are given in kcal/mol.

Al(III) zwitterion **QUI_4**. As the dearomatization of quinoline is involved in this step, it is the rate-determining step of this pathway. Subsequent coordination of another quinoline molecule to the electron-deficient Al(III) center in **QUI_4** leads to the hypervalent Al(III) species **QUI_5**. Finally, the two quinoline moieties in **QUI_5** undergo C—C coupling with a concurrent Al—C(8) bond cleavage, yielding the final product **QUI_P$_{trans}$**. Overall, this pathway has an energy barrier of 24.4 kcal/mol, which is much higher than the overall energy barrier presented in Figure 8.

To further support the hypothesis suggesting that the one-electron pathway is more favorable for the quinoline coupling reaction than the two-electron pathway, we have assessed the possibility of a [4+1] cycloaddition (Figure 11b,c). This pathway is based on a literature report that anionic Al(I) complexes can undergo reversible reactions with benzene through [4+1]

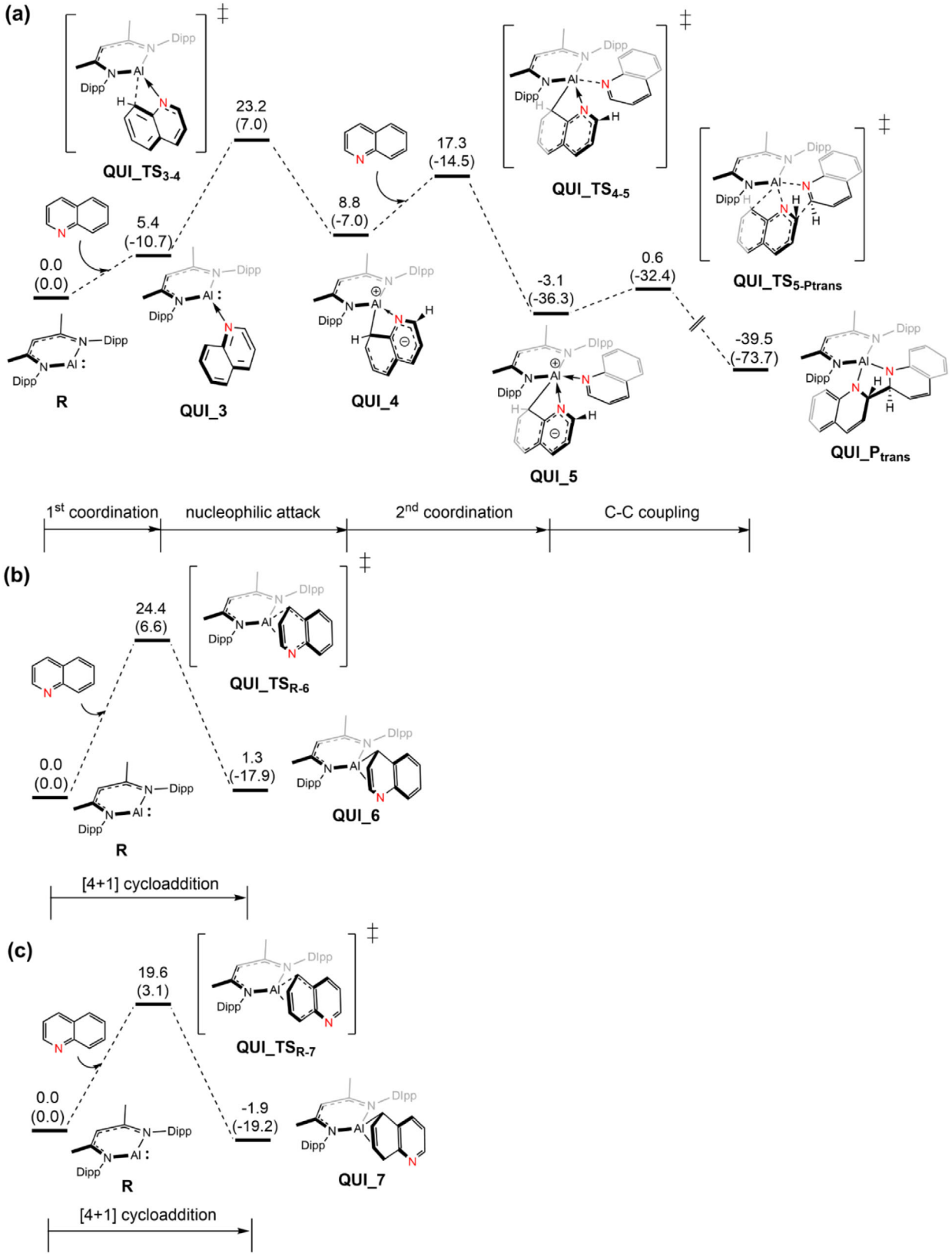

Figure 11. Energy profiles of other less favorable pathways for the reaction of NacNacAl(I) with quinoline: (a) intramolecular nucleophilic attack on the C(8) position of quinoline by Al(I) center of quinoline-NacNacAl(I) adduct, (b) [4+1] cycloaddition with quinoline at the N1 and C(4) positions by uncoordinated NacNacAl(I) and (c) [4+1] cycloaddition with quinoline at the C(5) and C(8) positions by uncoordinated NacNacAl(I). Relative free energies and electronic energies (in parentheses) are given in kcal/mol.

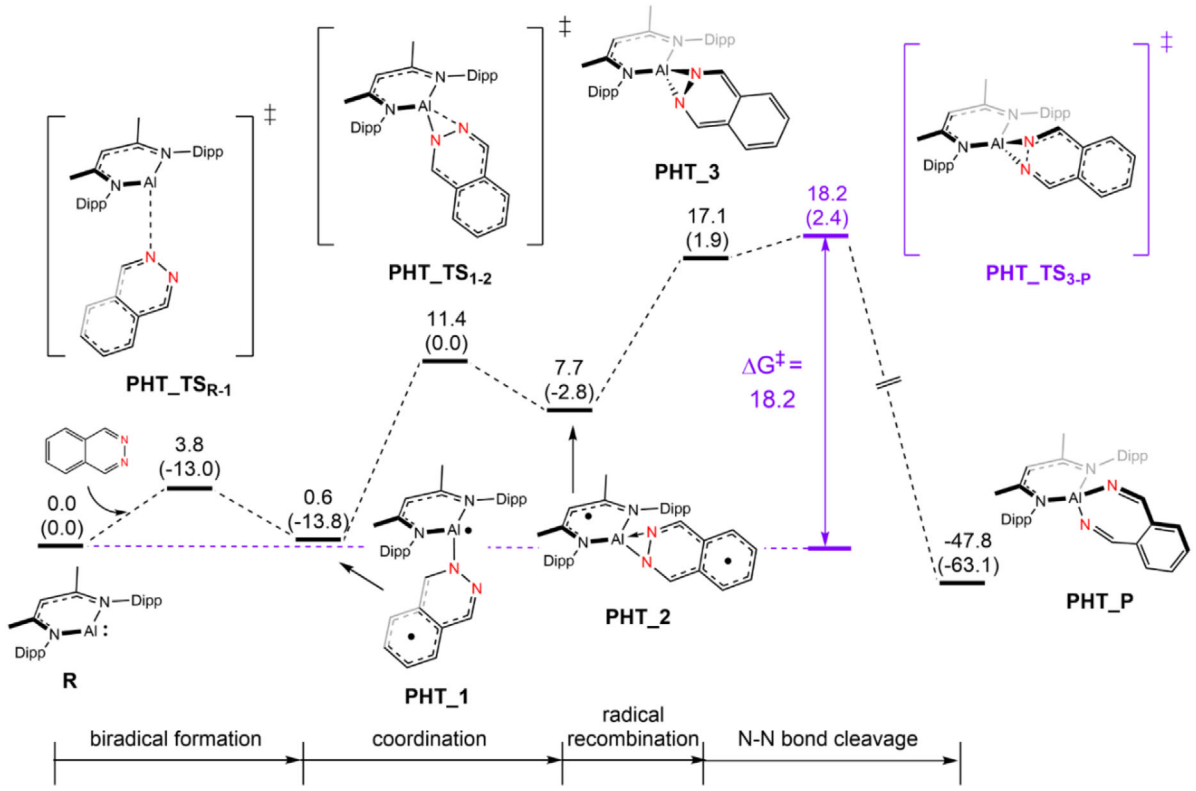

Figure 12. Energy profile calculated for the singlet biradical pathway for the reaction of NacNacAl(I) with phthalazine. Relative free energies and electronic energies (in parentheses) are given in kcal/mol.

cycloaddition.[58] Two possible pathways for the [4+1] cycloaddition were calculated, including the one undergoing [4+1] cycloaddition with quinoline at the N(1) and C(4) positions through **QUI_TS$_{R-6}$** as shown in Figure 11b, and another one at the C(5) and C(8) positions through **QUI_TS$_{R-7}$** as shown in Figure 11c. However, both pathways, with energy barriers of 24.4 kcal/mol for **QUI_TS$_{R-6}$** and 19.6 kcal/mol for **QUI_TS$_{R-7}$**, have higher barriers than the primary pathway presented in Figure 8.

2.2.2. N—N bond cleavage in phthalazine (PHT)

As phthalazine also contains an extensive π conjugate system similar to quinoline, the LUMO of phthalazine, π^* orbital of the π system, is also low-lying enough to comfortably accommodate an unpaired electron to form singlet biradical intermediates. However, in contrast to monodentate quinoline, phthalazine can act as a bidentate ligand to bind to the Al center, instead of coordinating two phthalazine molecules on the Al center. In addition, phthalazine has a relatively weak N—N bond labile for homolytic cleavage. Thus, a one-electron mechanism for cleavage of the N—N bond, instead of radical coupling, is realized for phthalazine.

As illustrated in Figure 12, phthalazine first coordinates with NacNacAl(I) to give the singlet biradical Al(II) intermediate **PHT_1**. As revealed by the SNO analysis,[56,57] the two unpaired electrons are separately distributed: one is delocalized in the π^* orbital of the coordinated phthalazine, while the other is located on the

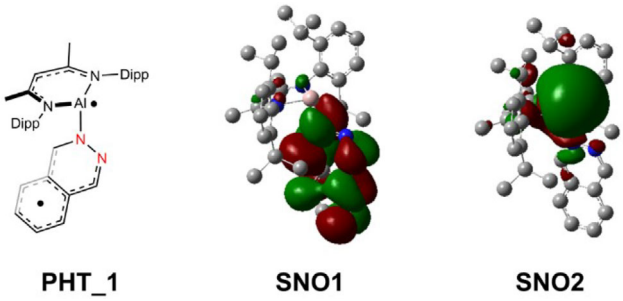

Figure 13. Spin natural orbitals calculated for the singlet biradical NacNacAl(I)-phthalazine adduct **PHT_1**.

sp^3-hybridized orbital of the Al(II) center (Figure 13). From **PHT_1**, coordination of the second N atom to the Al(II) center leads to the formation of another biradical species **PHT_2** having an Al(III) metal center. The frontier molecular orbital analysis of **PHT_2** (Figure S1, Supporting Information) indicates that, after this second N atom coordination, the unpaired electron at the Al(II) center shifts to the NacNac ligand. In other words, a concurrent intramolecular redox process occurs in which the NacNac ligand receives an unpaired electron from the Al(II) center, oxidizing the Al(II) center to Al(III). The next step of the mechanism involves a barrierless radical recombination in which the unpaired electron at the NacNac ligand recombines with the unpaired electron delocalized in the π system of the phthalazine moiety. The most significant structural changes from intermediate **PHT_2** to

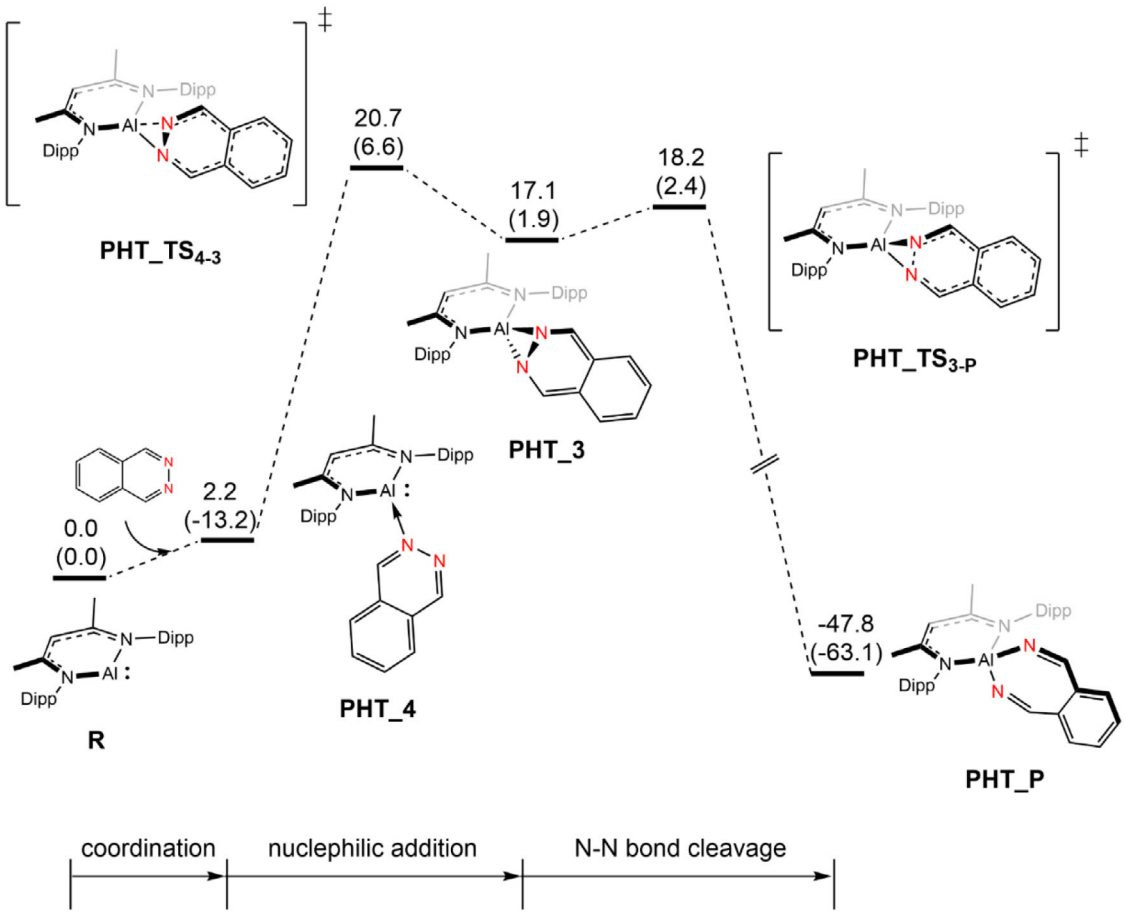

Figure 14. Energy profile of the less favorable pathway for the reaction of NacNacAl(I) with phthalazine: nucleophilic addition of NacNacAl(I) to phthalazine. Relative free energies and electronic energies (in parentheses) are given in kcal/mol.

the intermediate complex **PHT_3** are the lengthening of the N-N bond from 1.36 to 1.59 Å and the disruption of coplanarity between the plane encompassing the Al—N—N 3-membered ring and the plane encompassing the phthalazine ring. The weakening of the N-N bond facilitates the subsequent ring expansion (**PHT_TS$_{3\text{-}P}$**), yielding the final Al(III) product **PHT_P**. This rate-determining N—N bond cleavage gives an overall barrier of 18.2 kcal/mol for this reaction.

To validate the one-electron pathway discussed above, we also examined a two-electron pathway. In line with the previously discussed two-electron pathways, the coordination of phthalazine to NacNacAl(I) yields the Al(I) adduct **PHT_4** (Figure 14). The nucleophilicity of the lone pair at the Al(I) center is then enhanced, facilitating its subsequent nucleophilic addition to the phthalazine moiety at the other N atom through **PHT_TS$_{4\text{-}3}$**. The resulting reactive Al(III) species **PHT_3** is also a part of the primary pathway presented in Figure 12. Consequently, as discussed above, the N—N bond of intermediate **PHT_3** cleaves, yielding product **PHT_P**. The overall barrier for this pathway is 20.7 kcal/mol, which is higher than that of the primary pathway presented in Figure 12. Therefore, the one-electron pathway is again found to be more favorable for the cleavage of the N—N bond of phthalazine.

2.3. Monocyclic Versus Bicyclic Azaarenes

After discussing the one-electron pathways of bicyclic azaarenes, readers may question why similar one-electron pathways are not proposed in Section 2.1 regarding the reactions of monocyclic azaarenes. It can be accounted for by the size of the π system of azaarene which could affect the stability and accessibility of their singlet biradical intermediates. For bicyclic azaarenes, as they have a more extensive π system, the LUMO of azaarene, the π^* orbital, is low-lying enough that allows a smooth transfer of one electron from the Al(I) center to LUMO, forming a stable singlet biradical with two unpaired electrons on π system of azaarene ring and sp^3-hybridized orbital on the Al(II) center, respectively. As shown in Figure 15, the singlet biradical form is more stable than a non-radical adduct with both electrons paired in an sp^3-hybridized orbital on the Al(I) center, thus allowing the accessibility of one-electron pathway for bicyclic azaarenes. In contrast, for monocyclic azaarenes, as they have a smaller π system, the energy level of LUMO of monocyclic azaarenes is high that it either forbids or hinders the formation of singlet biradical intermediate. We further consolidate this idea from a thermodynamic perspective. The singlet biradical form of the NacNacAl(I)-monocyclic azaarenes was successfully located

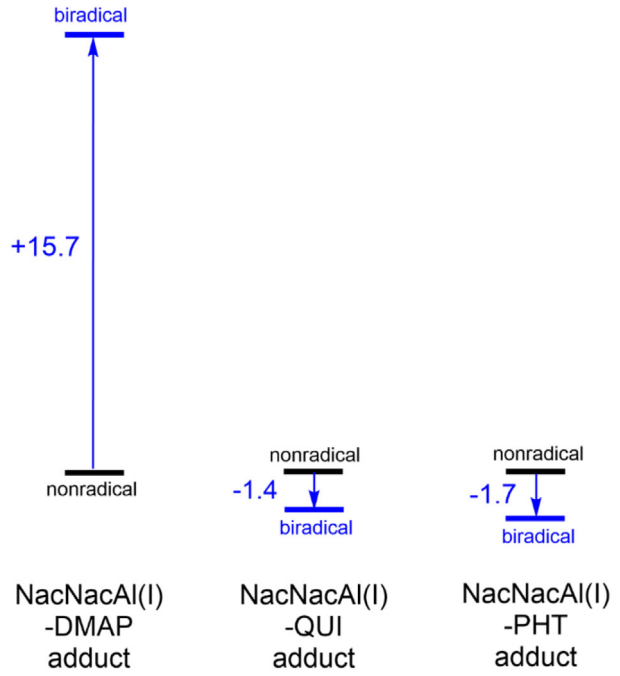

Figure 15. Relative free energies (kcal/mol) of the singlet biradical forms of the NacNacAl(I)-dimethylaminopyridine (DMAP) adduct, NacNacAl(I)-quinoline (QUI) adduct and NacNacAl(I)-phthalazine (PHT) adduct, with respect to their respective normal singlet states.

only when using the NacNacAl(I)-DMAP adduct. Furthermore, the singlet biradical state of NacNacAl(I)-DMAP is 15.7 kcal/mol higher in free energy than the normal singlet state (Figure 15). Hence, the singlet biradical state is not favorable for monocyclic azaarenes, and thus one-electron pathway is not favorable for monocyclic azaarenes.

3. Conclusion

Through our DFT calculations, we have established a collection of mechanisms for the reactions of NacNacAl(I) with five different azaarenes: 3,5-lutidine, 4-picoline, DMAP, quinoline, and phthalazine, each yielding distinctly different products. Our findings indicate that the three monocyclic azaarenes, 3,5-lutidine, 4-picoline, and DMAP, initially form adducts with NacNacAl(I), proceeding nucleophilic attack or deprotonation by leveraging the Al(I) center's lone pair of electrons, manifesting as either nucleophiles or Brønsted bases. In contrast, the two bicyclic azaarenes, quinoline, and phthalazine, initiate the process by generating biradical species upon coordinating to NacNacAl(I). These biradical species then follow one-electron pathways, involving concurrent coordination and oxidation of the Al(II) center.

Building upon the above-mentioned general understanding of the reaction mechanisms, we now proceed with further elaboration. The role of NacNacAl(I) is to act as a Lewis acid and initiate the reactions by coordinating nitrogen of azaarenes to the Al(I) center of NacNacAl(I). This coordination can lead to the formation of either a Lewis acid-base adduct or a biradical species. We also confirmed that the NacNac ligand can serve as a Brønsted acid, undergoing β-methyl deprotonation by a strong base.

For bicyclic azaarenes, such as quinoline and phthalazine, their π systems are sufficiently large. Coordination of a bicyclic azaarene to NacNacAl(I) results in the formation of the NacNacAl(I)-azaarene singlet biradical species in which one unpaired electron is associated with the azaarene π system (received from the azaarene-coordinated Al(I) center) and the other unpaired electron is located on the Al(II) center. Therefore, the reactions follow one-electron pathways.

For substituted monocyclic azaarenes, such as 4-picoline, 3,5-lutidine, DMAP, the substituent at the 4-position of the aromatic ring is also crucial in determining their reactivity. When the 4-position substituent possesses a C—H bond at the atom α to the aromatic ring, its deprotonation is promoted. In contrast, when there is no electron-donating substituent at the 4-position, the azaarene can act as an electrophile, susceptible to the nucleophilic attack of NacNacAl(I)-azaarene adducts. In both scenarios, a negative charge is developed at the carbon atom adjacent to the C(4) position. This results in the most stable resonance structure, with the negative charge residing on the electronegative nitrogen atom of the azaarene moiety, which offers additional stabilization through increased coordination of the nitrogen atom to the Al center.

4. Computational Details

All the density functional theory (DFT) calculations were conducted using Gaussian 09 (rev. D.01).[57] All of the structures were optimized (inclusion of solvent effects) using the Becke3PW91 (B3PW91) functional.[59,60] For Al atoms, the Stuttgart SDDAll effective core potential (ECP) and associated basis sets were employed, while the 6–31G(d,p) basis set was used for all other atoms.[61–63] The solvation model based on solute electron density (SMD),[64] which is more suitable for non-polar solvents, was applied, with benzene as the solvent for reaction involving the DMAP substrate and toluene as the solvent for reaction involving the phthalazine substrate. For other reactions, the polarizable continuum model (PCM),[65] which is more suitable for polar solvents, was used, with diethyl ether defined as the solvent. Dispersion corrections were also applied during the optimization using Grimme's D3 correction.[66] Vibrational frequency calculations were performed to ensure that the optimized intermediates do not possess imaginary frequencies and transition states only possess one imaginary frequency. Intrinsic reaction coordinate (IRC) calculations were also conducted to further confirm the transition states.[67,68] NBO version 3.1 was used to generate the SNO plots.[69]

Supporting Information

Supplementary plots of energy profile for the H/D Exchange of **PIC_P**, SNOs of **QUI_2** and **PHT_2**, table of energies of the stationary points are included in Supporting Information. Cartesian

coordinates of all the stationary points are included in an XYZ file.

Acknowledgments

This work was supported by the Research Grants Council of Hong Kong (HKUST 16301823).

Conflict of Interest

The authors declare no conflicts of interest.

Data Availability Statement

The data that support the findings of this study are available in the supplementary material of this article.

Keywords: aluminum(I) complexes · biradical singlets · density functional calculations · nitrogen heterocycles · reaction mechanisms

[1] C. Dohmeier, C. Robl, M. Tacke, H. Schnöckel, *Angew. Chem., Int. Ed.* **1991**, *30*, 564.
[2] C. Cui, H. W. Roesky, H. G. Schmidt, M. Noltemeyer, H. Hao, F. Cimpoesu, *Angew. Chem.* **2000**, *39*, 4274.
[3] J. D. Queen, A. Lehmann, J. C. Fettinger, H. M. Tuononen, P. P. Power, *J. Am. Chem. Soc.* **2020**, *142*, 20554.
[4] X. Zhang, L. L. Liu, *Angew. Chem., Int. Ed.* **2021**, *60*, 27062.
[5] A. Hinz, M. P. Müller, *Chem. Commun.* **2021**, *57*, 12532.
[6] A. Hofmann, T. Tröster, T. Kupfer, H. Braunschweig, *Chem. Sci.* **2019**, *10*, 3421.
[7] G. Tan, T. Szilvási, S. Inoue, B. Blom, M. Driess, *J. Am. Chem. Soc.* **2014**, *136*, 9732.
[8] D. Dhara, A. Jayaraman, M. Härterich, R. D. Dewhurst, H. Braunschweig, *Chem. Sci.* **2022**, *13*, 5631.
[9] A. Saddington, S. Dong, S. Yao, J. Zhu, M. Driess, *Angew. Chem., Int. Ed.* **2024**, *63*, e202410790.
[10] S. K. Mellerup, Y. Cui, F. Fantuzzi, P. Schmid, J. T. Goettel, G. Bélanger-Chabot, M. Arrowsmith, I. Krummenacher, Q. Ye, V. Engel, B. Engels, H. Braunschweig, *J. Am. Chem. Soc.* **2019**, *141*, 16954.
[11] J. D. Gorden, A. Voigt, C. L. B. Macdonald, J. S. Silverman, A. H. Cowley, *J. Am. Chem. Soc.* **2000**, *122*, 950.
[12] C. Dohmeier, H. Krautscheid, H. Schnöckel, *Angew. Chem., Int. Ed.* **1995**, *33*, 2482.
[13] D. Weiss, T. Steinke, M. Winter, R. A. Fischer, N. Fröhlich, J. Uddin, G. Frenking, *Organometallics* **2000**, *19*, 4583.
[14] S. Schulz, T. Schoop, H. W. Roesky, L. Häming, A. Steiner, R. Herbst-Irmer, *Angew. Chem., Int. Ed.* **1995**, *34*, 919.
[15] C. K. F. von Hänisch, C. Üffing, M. A. Junker, A. Ecker, B. O. Kneisel, H. Schnöckel, *Angew. Chem.* **1996**, *108*, 3003.
[16] C. Dohmeier, H. Schnöckel, C. Robl, U. Schneider, R. Ahlrichs, *Angew. Chem.* **1994**, *106*, 225.
[17] S. Schulz, A. Voigt, H. W. Roesky, L. Häming, R. Herbst-Irmer, *Organometallics* **1996**, *15*, 5252.
[18] S. Schulz, L. Häming, R. Herbst-Irmer, H. W. Roesky, G. M. Sheldrick, *Angew. Chem., Int. Ed.* **1994**, *33*, 969.
[19] M. Fischer, S. Nees, T. Kupfer, J. T. Goettel, H. Braunschweig, C. Hering-Junghans, *J. Am. Chem. Soc.* **2021**, *143*, 4106.
[20] S. Schulz, H. W. Roesky, H. J. Koch, G. M. Sheldrick, D. Stalke, A. Kuhn, *Angew. Chem., Int. Ed.* **1993**, *32*, 1729.
[21] M. R. Crimmin, M. J. Butler, A. J. P. White, *J. Chem. Soc., Chem. Commun.* **2015**, *51*, 15994.
[22] D. Dhara, A. Jayaraman, M. Härterich, M. Arrowsmith, M. Jürgensen, M. Michel, H. Braunschweig, *Chem. – Eur. J.* **2023**, *29*, e202300483.
[23] J. D. Queen, S. Irvankoski, J. C. Fettinger, H. M. Tuononen, P. P. Power, *J. Am. Chem. Soc.* **2021**, *143*, 6351.
[24] X. Zhang, L. L. Liu, *Eur. J. Inorg. Chem.* **2023**, *26*, e202300157.
[25] S. Grams, J. Mai, J. Langer, S. Harder, *Organometallics* **2022**, *41*, 2862.
[26] S. Nagendran, H. W. Roesky, *Organometallics* **2008**, *27*, 457.
[27] X. Zhang, Z. Cao, *Dalton Trans.* **2016**, *45*, 10355.
[28] C. Bakewell, A. J. P. White, M. R. Crimmin, *Angew. Chem.* **2018**, *130*, 6748.
[29] S. Grams, J. Eyselein, J. Langer, C. Färber, S. Harder, *Angew. Chem., Int. Ed.* **2020**, *59*, 15982.
[30] X. Zhang, L. L. Liu, *J. Am. Chem. Soc.* **2023**, *145*, 15729.
[31] S. Ahmed, I. Fernández, A. K. Phukan, *Dalton Trans.* **2023**, *52*, 8567.
[32] J. Hicks, P. Vasko, J. M. Goicoechea, S. Aldridge, *Nature* **2018**, *557*, 92.
[33] R. J. Schwamm, M. D. Anker, M. Lein, M. P. Coles, *Angew. Chem., Int. Ed.* **2018**, *58*, 1489.
[34] R. J. Schwamm, M. P. Coles, M. S. Hill, M. F. Mahon, C. L. McMullin, N. A. Rajabi, A. S. S. Wilson, *Angew. Chem., Int. Ed.* **2020**, *59*, 3928.
[35] S. Kurumada, S. Takamori, M. Yamashita, *Nat. Chem.* **2019**, *12*, 36.
[36] K. Koshino, R. Kinjo, *J. Am. Chem. Soc.* **2020**, *142*, 9057.
[37] T. Chu, I. Korobkov, G. I. Nikonov, *J. Am. Chem. Soc.* **2014**, *136*, 9195.
[38] S. Jain, K. Vanka, *Chem. – Eur. J.* **2017**, *23*, 13957.
[39] T. Chu, Y. Boyko, I. Korobkov, G. I. Nikonov, *Organometallics* **2015**, *34*, 5363.
[40] C. E. Pitsch, X. Wang, *J. Chem. Soc., Chem. Commun.* **2017**, *53*, 8196.
[41] X. Zhang, P. Li, B. Wang, Z. Cao, *Front. Chem.* **2019**, *7*, 596.
[42] T. Chu, Y. Boyko, I. Korobkov, L. G. Kuzmina, J. A. K. Howard, G. I. Nikonov, *Inorg. Chem.* **2016**, *55*, 9099.
[43] H. Zhu, J. Chai, H. Fan, H. W. Roesky, U. N. Nehete, H.-G. Schmidt, M. Noltemeyer, *Eur. J. Inorg. Chem.* **2005**, *2005*, 2147.
[44] C. Bakewell, A. J. P. White, M. R. Crimmin, *Chem. Sci.* **2019**, *10*, 2452.
[45] H. Zhu, J. Chai, H. Fan, H. W. Roesky, C. He, V. Jancik, H.-G. Schmidt, M. Noltemeyer, W. A. Merrill, P. P. Power, *Angew. Chem., Int. Ed.* **2005**, *44*, 5090.
[46] W. W. Schoeller, G. D. Frey, *Inorg. Chem.* **2016**, *55*, 10947.
[47] T. Chu, S. F. Vyboishchikov, B. M. Gabidullin, G. I. Nikonov, *J. Am. Chem. Soc.* **2017**, *139*, 8804.
[48] C. Bakewell, M. Garçon, R. Y. Kong, L. O'Hare, A. J. P. White, M. R. Crimmin, *Inorg. Chem.* **2020**, *59*, 4608.
[49] S. R. Lawrence, T. Rüffer, A. Stasch, R. Kretschmer, *J. Chem. Soc., Chem. Commun.* **2023**, *59*, 7923.
[50] A. Dmitrienko, M. Pilkington, J. F. Britten, B. M. Gabidullin, A. van der Est, G. I. Nikonov, *Angew. Chem., Int. Ed.* **2020**, *59*, 16147.
[51] Y. García-Rodeja, F. M. Bickelhaupt, I. Fernández, *Chem. – Eur. J.* **2016**, *22*, 13669.
[52] C. Camp, J. Arnold, *Dalton Trans.* **2016**, *45*, 14462.
[53] T. Chu, S. F. Vyboishchikov, B. M. Gabidullin, G. I. Nikonov, *Inorg. Chem.* **2017**, *56*, 5993.
[54] M. Abe, J. Ye, M. Mishima, *Chem. Soc. Rev.* **2012**, *41*, 3808.
[55] W. W. Schoeller, G. D. Frey, *Inorg. Chem.* **2014**, *53*, 4840.
[56] F. K. Sheong, J.-X. Zhang, Z. Lin, *J. Comput. Chem.* **2019**, *40*, 1172.
[57] M. J. Frisch, G. W. Trucks, H. B. Schlegel, G. E. Scuseria, M. A. Robb, J. R. Cheeseman, G. Scalmani, V. Barone, G. A. Petersson, H. Nakatsuji, X. Li, M. Caricato, A. Marenich, J. Bloino, B. G. Janesko, R. Gomperts, B. Mennucci, H. P. Hratchian, J. V. Ortiz, A. F. Izmaylov, J. L. Sonnenberg, D. Williams-Young, F. Ding, F. Lipparini, F. Egidi, J. Goings, B. Peng, A. Petrone, T. Henderson, D. Ranasinghe, et al., *Gaussian09, Revision D.01*, Gaussian, Inc., Wallingford, CT **2009**.
[58] D. Sarkar, P. Vasko, A. F. Roper, A. E. Crumpton, M. M. D. Roy, L. P. Griffin, C. Bogle, S. Aldridge, *J. Am. Chem. Soc.* **2024**, *146*, 11792.
[59] K. Burke, J. P. Perdew, and Y. Wang, *Electronic Density Functional Theory: Recent Progress and New Directions*, (Eds: J. F. Dobson, G. Vinnale, M. P. Das), Plenum, New York, **1998**.
[60] J. P. Perdew, K. Burke, Y. Wang, *Phys. Rev. B* **1996**, *54*, 16533.
[61] W. J. Hehre, R. Ditchfield, J. A. Pople, *J. Chem. Phys.* **1972**, *56*, 2257.
[62] P. C. Hariharan, J. A. Pople, *Theor. Chim. Acta* **1973**, *28*, 213.

[63] T. Clark, J. Chandrasekhar, G. W. Spitznagel, P. V. R. Schleyer, *J. Comput. Chem.* **1983**, *4*, 294.
[64] A. V. Marenich, C. J. Cramer, D. G. Truhlar, *J. Phys. Chem. B* **2009**, *113*, 6378.
[65] J. Tomasi, B. Mennucci, R. Cammi, *Chem. Rev.* **2005**, *105*, 2999.
[66] S. Grimme, J. Antony, S. Ehrlich, H. Krieg, *J. Chem. Phys.* **2010**, *132*, 154104.
[67] K. Fukui, *Acc. Chem. Res.* **1981**, *14*, 363.
[68] K. Fukui, *J. Phys. Chem.* **1970**, *74*, 4161.
[69] E. D. Glendening, A. E. Reed, J. E. Carpenter, F. Weinhold, *NBO Version 3.1*, University of Wisconsin, Madison, WI **1990**.

Manuscript received: March 1, 2025
Revised manuscript received: March 26, 2025
Version of record online: April 21, 2025